Free-surface flows with near-critical flow conditions

H. Chanson

Abstract: Open channel flow situations with near-critical flow conditions are often characterized by the development of free-surface instabilities (i.e., undulations). The paper develops a review of several near-critical flow situations. Experimental results are compared with ideal-fluid flow calculations. The analysis is completed by a series of new experiments. The results indicate that, for Froude numbers slightly above unity, the free-surface characteristics are very similar. However, with increasing Froude numbers, distinctive flow patterns develop.

Key words: open channel flow, critical flow conditions, free-surface undulations, flow instability, undular surge, undular broad-crested weir flow, culvert flow.

Résumé : Pour des écoulements à surface libre, les conditions d'écoulement critique sont souvent caractérisées par des instabilités de la surface libre (c.-à-d. des ondulations). L'auteur présente une revue de plusieurs types d'écoulements quasi-critiques. On compare des résultats expérimentaux avec des calculs de fluides parfaits. L'auteur présente aussi de nouveaux résultats expérimentaux. Les résultats montrent que, pour des nombres de Froude légérement supérieurs à un, les caractéristiques des ondulations sont très similaires. Par contre, pour de nombres de Froude plus importants, chaque type d'écoulements développe des caractéristiques distinctives.

Mots clés : ecoulement à surface libre, conditions d'écoulement critique, ondulations de la surface libre, instabilité de l'écoulement, onde de translation, déversoir à seuil large, culvert.

1. Introduction

Near-critical flows are characterized by the occurrence of critical or nearly-critical flow conditions over a reasonably long distance and period of time. At critical flow conditions,[1] the relationship between specific energy and flow depth (e.g., Henderson 1966) is characterized by an infinitely large change of flow depth for a very small change of energy. A small change of flow energy can be caused by a bottom or sidewall irregularity, by turbulence generated in the boundary layers, or by an upstream disturbance. The unstable nature of near-critical flows is favourable to the development of large free-surface undulations.

In this paper, it is proposed to review several near-critical flows: undular surges, undular flow above broad-crested weir, free-surface undulations downstream of backward-facing step, and undulations in rectangular-cross-section culvert (Fig. 1). The flow characteristics are compared with undular hydraulic jump flows (Chanson 1993, 1995; Chanson and Montes 1995). New qualitative experiments were performed to complete the analysis.

It must be emphasized that other types of near-critical flows may occur than those described in the paper. In particular, the reader may wish to consult some Soviet investigations, including Gordienko (1968), Kurganov (1974), and Tursunov (1969).

Received November 8, 1995.
Revised manuscript accepted June 24, 1996.

H. Chanson. Department of Civil Engineering, The University of Queensland, Brisbane QLD 4072, Australia.

Written discussion of this paper is welcomed and will be received by the Editor until April 30, 1997 (address inside front cover).

[1] Flow conditions such that the specific energy is minimum are called critical flow conditions.

2. Undular surge (travelling bore)

2.1. Presentation

A (positive) surge wave results from a sudden increase in flow depth (e.g., caused by a partial gate closure). As seen by an observer travelling at the surge speed C_s, a (positive) surge is a quasi-steady-flow situation. When the ratio of the sequent depths is close to unity, free-surface undulations develop downstream of the surge front called an undular surge flow (Tables 1 and 2).

2.2. Wave characteristics

Several theoretical calculations of wave characteristics (e.g., amplitude and length) were developed since the 19th century. Among these, two studies proposed a simple form of solutions. Keulegan and Patterson (1940) analysed the irrotational translation of a solitary wave. The solution shows the existence of an infinite number of undulations of identical size and shape called cnoidal waves. By equating the propagation velocity of the centre of gravity of the solitary wave to that of the wave train itself, they obtained the following:

$$[1a]\quad \Delta d = \frac{1}{2}(d_2 - d_1)$$

$$[1b]\quad \frac{\Delta d}{d_c} = \frac{\sqrt{1 + 8\mathrm{Fr}_1^2} - 3}{4\mathrm{Fr}_1^{2/3}}$$

where d_1 and d_2 are the upstream and downstream depths, d_c is the critical depth, and Δd is the height of the initial undulation. For the experiments of Bazin (1865), Keulegan and Patterson (1940) correlated the wave amplitude data as $\Delta d = (0.61 \pm 0.18)(d_2 - d_1)$ which is close to [1a].

Table 1. Conditions of existence of undular surges (travelling bores).

Reference	Condition for undular surge flow	Remarks
Favre (1935)	$d_2/d_1 < 1.28$	Laboratory experiments; rectangular cross section ($W = 0.42$ m); zero initial velocity ($V_1 = 0$)
Rouse (1938)	$d_2/d_1 < 2$	
Henderson (1966)	$d_2/d_1 < 1.35$ to 1.95	1.35 for smooth channel; 1.95 for rough channel
Benet and Cunge (1971)	$d_2/d_1 < 1.29$ for $V_1 = 0$ $d_2/d_1 < 1.35$ for $0 < V_1/\sqrt{gd_1} < 0.1$ $d_2/d_1 < 1.37$ for $V_1/\sqrt{gd_1} > 0.1$	Laboratory experiments in trapezoidal channel (see Table 2)
Treske (1994)	$Fr_1 < 1.38$ ($d_1 = 0.16$ m) $Fr_1 < 1.34$ ($d_1 = 0.08$ m)	Laboratory experiments in rectangular channel (see Table 2)
	$Fr_1 < 1.33$	Laboratory experiments in trapezoidal channel (see Table 2)

Table 2. Experimental investigations of undular surges (travelling bores).

Reference	Initial flow		Surge type*	Channel geometry	Remarks
	V_1 (m/s)	d_1 (m)			
Favre (1935)[†]	0	0.106–0.206	+U/S	Rectangular ($W = 0.42$ m); $\alpha = 0°$	Laboratory experiments; flume length = 73.8 m
	0	0.109–0.265	+U/S	Rectangular ($W = 0.42$ m); $\alpha = 0.017°$	
Zienkiewicz and Sandover (1957)		0.05–0.11	+	Rectangular ($W = 0.127$ m); $\alpha = 0°$; smooth flume: glass; rough flume: wire mesh	Laboratory experiments: flume length = 12.2 m
Benet and Cunge (1971)	0–0.198	0.057–0.138	+D/S	Trapezoidal (base width = 0.172 m; sideslope = 2H:1V); $\alpha = 0.021°$	Laboratory experiments; flume length = 32.5 m
	0.59–1.08	6.61–9.16	+U/S	Trapezoidal (base width = 9 m; sideslope = 2H:1V); $\alpha = 0.006–0.0086°$	Oraison power plant intake channel
	1.51–2.31	5.62–7.53	+U/S	Trapezoidal (base width = 8.6 m; sideslope = 2H:1V)	Jouques-Saint Estève intake channel
Treske (1994)		0.08–0.16	+U/S	Rectangular ($W = 1$ m); $\alpha = 0.001°$	Laboratory experiments; flume length = 100 m; concrete channel
		0.04–0.16	+U/S, +D/S, −	Trapezoidal (base width = 1.24 m; sideslope = 3H:1V); $\alpha = 0°$	Laboratory experiments; flume length = 124 m; concrete channel
Present study	0.4–1.2	0.02–0.15	+U/S	Rectangular ($W = 0.25$ m); $\alpha = 0.19–0.54°$	Laboratory experiments; flume length = 20 m

*Surge type: +, positive surge; −, negative surge; U/S, moving upstream; D/S, moving downstream.
[†] See also Benet and Cunge (1971).

Andersen (1978) developed the Boussinesq energy equation (Boussinesq 1871, 1877) as

$$[2] \quad E_1 = d + \frac{V^2}{2g}\left(1 + \frac{2}{3}d\frac{\partial^2 d}{\partial x^2}\right)$$

where E_1 is the upstream specific energy, V is the velocity, and d is the flow depth. Using the continuity equation, neglecting the energy losses, and integrating [2], the wave amplitude is the solution of

$$[3] \quad 3\frac{E_1}{d_c}\left[\left(\frac{d_2 + \Delta d}{d_c}\right)^2 - \left(\frac{d_1}{d_c}\right)^2\right] - 2\left[\left(\frac{d_2 + \Delta d}{d_c}\right)^3 - \left(\frac{d_1}{d_c}\right)^3\right] - 3\ln\left(\frac{d_2 + \Delta d}{d_1}\right) = 0$$

To a first approximation, [1] and Δd satisfying [3] can be correlated respectively by

Fig. 1. Sketch of near-critical undular flows: (A) undular surges; (B) undular flow at weirs; (C) undular flow downstream of drop; (D) undular flows downstream of impinging jet; (E) undular flows downstream of submerged bodies; and (F) undular flows developing above wake and shear flow regions.

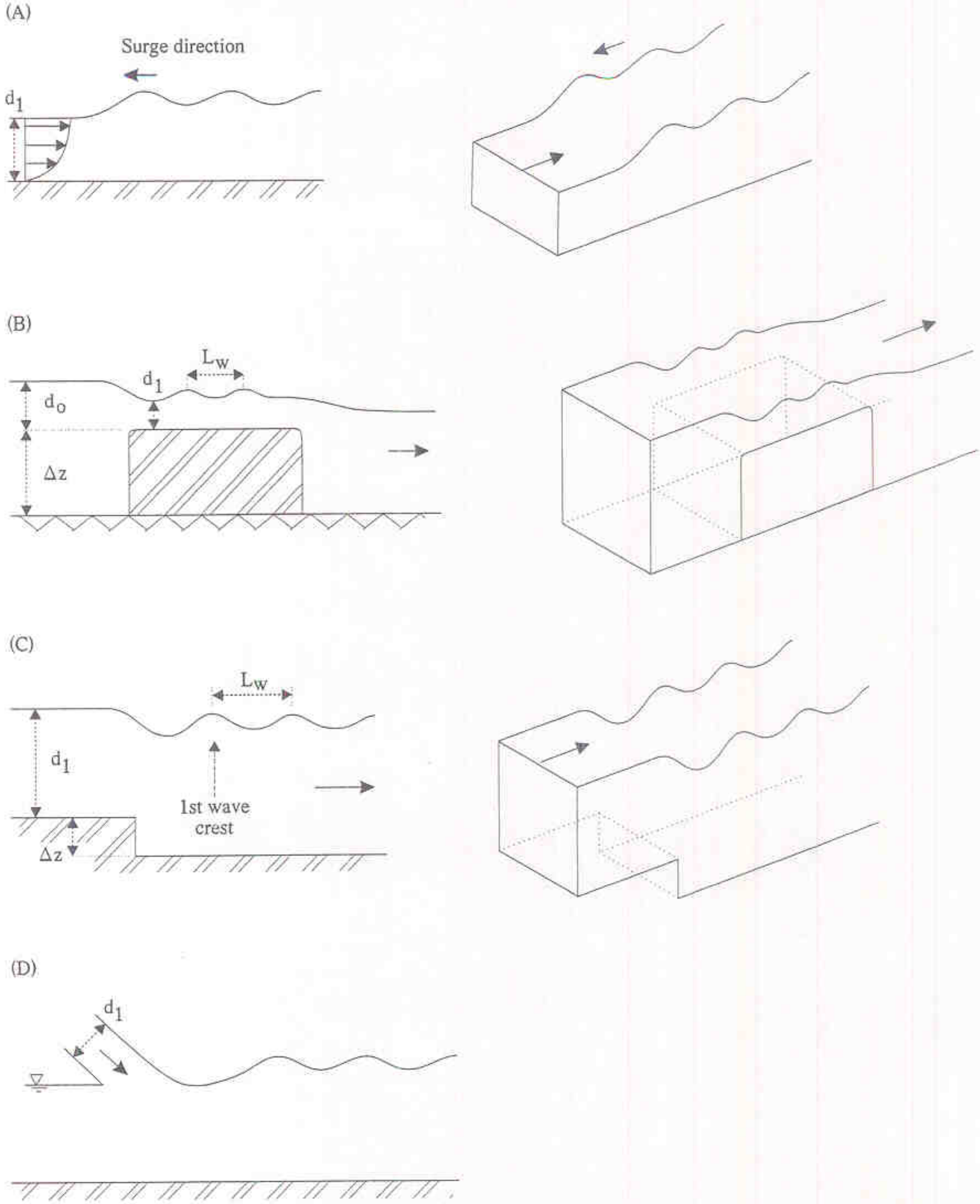

– Keulegan and Patterson's theory:

$$\frac{\Delta d}{d_c} = 0.515(\mathrm{Fr}_1 - 1)^{0.932} \quad [4]$$

– Andersen's theory:

$$\frac{\Delta d}{d_c} = 0.741(\mathrm{Fr}_1 - 1)^{1.028} \quad [5]$$

The theories of Andersen (1978) and Keulegan and Patterson (1940) give similar results for Froude numbers close to unity. They differ, however, for Froude numbers[2] larger than 1.3 (Fig. 2). Compared with experimental data (Fig. 2), both theories underestimate slightly the wave amplitude. Note that the data of Benet and Cunge (1971) and Treske (1994) are the *sidewall* amplitudes. In trapezoidal channels (model and field data) and in natural streams (Tricker 1965), the wave

[2] The Froude number is defined such that Fr = 1 when the specific energy is minimum.

Fig. 1 (*concluded*).

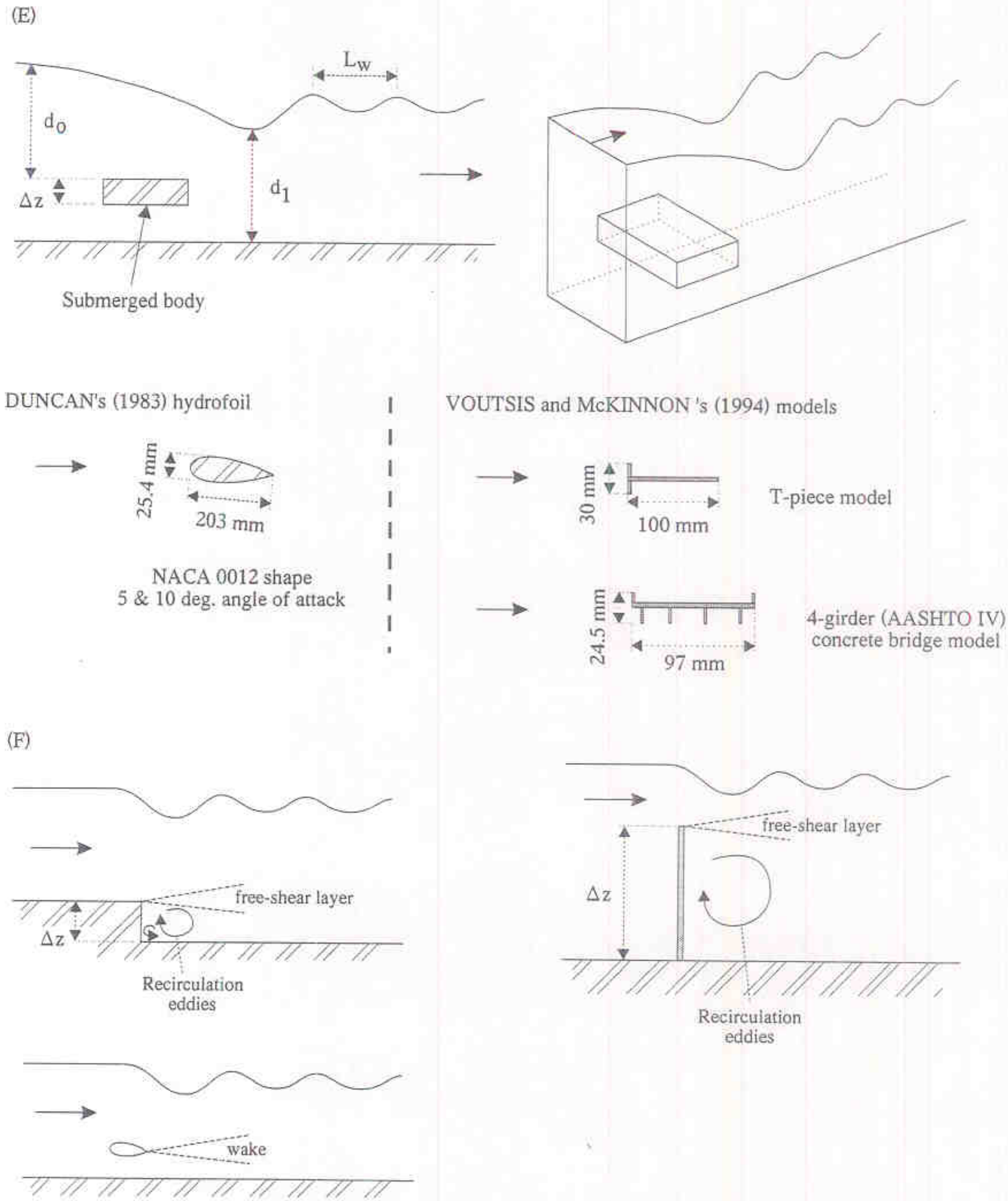

amplitude at the banks is larger than on the centreline.

It is worth noting that the wave amplitude decreases sharply immediately before the wave breaking, as shown by the data of Treske (1994) (Fig. 2), in a manner similar to undular hydraulic jumps (Chanson and Montes 1995).

For wave amplitudes that are small compared with the downstream flow depth, the linearization of the Boussinesq energy equation yields (Andersen 1978)

$$[6] \quad \frac{L_w}{d_c} = \frac{\pi(\sqrt{1 + 8\mathrm{Fr}_1^2} - 1)}{\sqrt{3\mathrm{Fr}_1^3\left[\frac{1}{8\mathrm{Fr}_1^2}(\sqrt{1 + 8\mathrm{Fr}_1^2} - 1)^3 - 1\right]}}$$

Equation [6] can be simplified as

$$[7] \quad \frac{L_w}{d_c} = \frac{3.15}{(\mathrm{Fr}_1 - 1)^{0.45}}$$

Andersen's theory is compared with some experimental data in Fig. 3. For trapezoidal channels and for rough boundaries, the data follow the general trend with some scatter.

2.3. Discussion: new undular surge experiments

The author performed several undular surge experiments in the flume used by Chanson and Montes (1995). The same procedure was used each time for various discharges and chan-

Fig. 2. Undular surge: wave amplitude $\Delta d/d_c$ as a function of the upstream Froude number Fr_1. Comparison between the theories of Keulegan and Patterson (1940), Andersen (1978) and experimental data (Table 2).

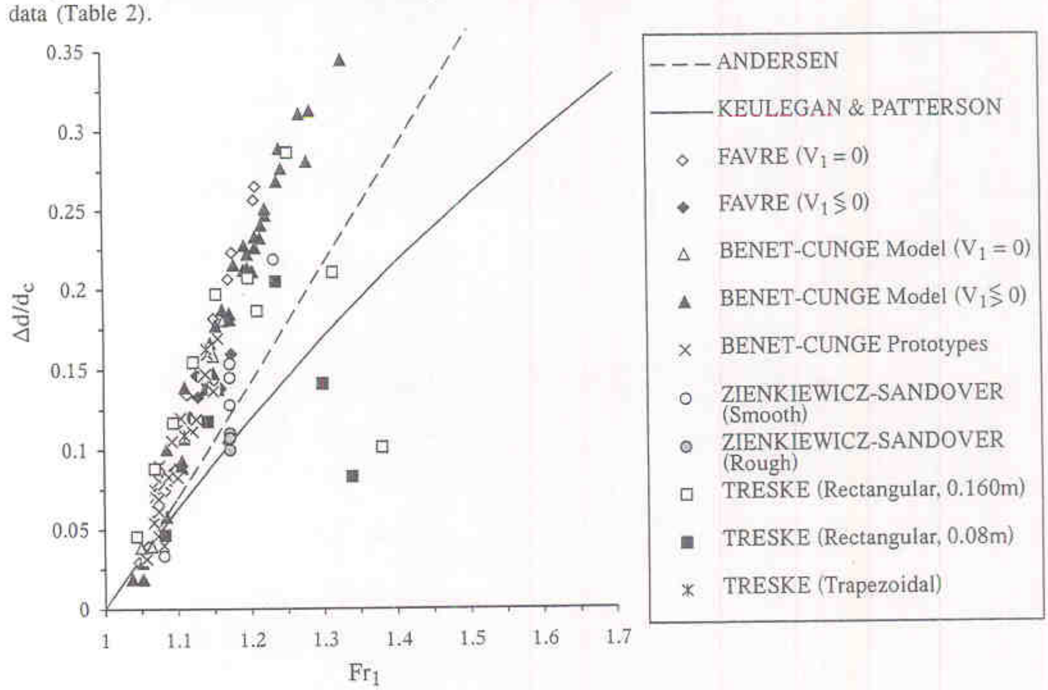

Fig. 3. Undular surge: dimensionless wavelength as a function of the upstream Froude number Fr_1. Comparison between Andersen's (1978) theory and experimental data (Table 2).

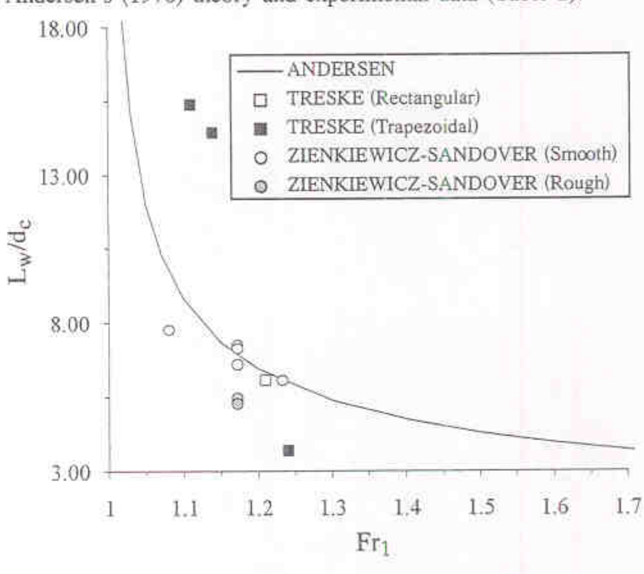

nel slopes. Near-critical (super- and sub-critical) uniform flows were established in the flume. Then the downstream gate was closed partially. The travelling surge moved upstream against the uniform flow (i.e., fully developed boundary layer flow) and was allowed to travel over the 20-m flume length.

In each case, the surge wave front was two-dimensional, except in rare cases discussed below. For an observer moving with the surge, the free-surface profile appeared stationary. Such observations confirm clearly the differences of flow pattern between undular surges and undular jumps observed in the same experimental facility.

In rare cases a weak undular surge would stop before the channel upstream end. It would become an undular jump after a long period of typically 5 − 10 min. Visual observations indicate that, when the surge celerity falls below a critical value of around a few centimetres per second, the surge flow would then start becoming three-dimensional. And it would take up to 20 min before the surge front is stable and stationary to develop the distinctive three-dimensional flow patterns of undular jumps (Chanson and Montes 1995).

3. Undular flow above a broad-crested weir

3.1. Introduction

A broad-crested weir is a flat-crested structure (Fig. 1B). When the crest is long enough to maintain nearly hydrostatic pressure distribution within the flow across the weir, critical flow conditions occur on the crest. The hydraulic characteristics of broad-crested weirs were studied during the 19th and 20th centuries. Hager and Schwalt (1994) presented recently a remarkable authoritative study.

3.2. Undular weir flow

For low discharges (i.e., $d_0/\Delta z$ small), several researchers observed free-surface undulations above the crest of broad-crested weir (Table 3). In their recent investigations, Hager and Schwalt (1994) indicated that the undular weir flow occurred for

[8] $\quad Fr_1 < 1.5$

where the subscript 1 refers to the minimum flow depth on the crest (Fig. 1B).

The author investigated qualitatively the flow pattern of undular weir flow in a glass flume at the University of Queensland. The flume width is 0.25 m, the sill height is 0.0646 m,

Table 3. Undular flow conditions above broad-crested weirs.

Reference	d_c/W	Flow conditions	Remarks
Govinda Rao and Muralidhar (1963)		Define Fr_1 such that the head on crest to weir length ratio is less than 0.1	
Bos (1976)		Define Fr_1 such that the head on crest to weir length ratio is less than 0.08	
Hager and Schwalt (1994)	0.033−0.073	$Fr_1 < 1.5$*	Laboratory experiments (see Table 4)

*Corresponding to a head on crest to weir length ratio of less than 0.102.

Table 4. Summary of experimental flow conditions — undular weir flows.

Reference	Q_w (L/s)	Fr_1	d_c/W	Comments
Woodburn (1932)	4.8−7.6	0.86−1.09	0.096−0.131	$W = 0.305$ m
Tison (1950)	39.6−45.9	0.91−1.30	0.172−0.190	$W = 0.5$ m; data reanalysed by Serre (1953)
Hager and Schwalt (1994)	3.15−8.25	1.19−1.45	0.032−0.061	$W = 0.499$ m; $\Delta z = 0.401$ m; crest length = 0.5 m
Present study	Up to 4			$W = 0.25$ m; $\Delta z = 0.0646$ m; crest length = 0.42 m; substantial effect of the developing boundary layer (see Isaacs 1981)

the horizontal crest length is 0.42 m, and the crest has a rounded upstream edge (28-mm radius) and a tapered down-slope (concave upwards). Visual observations indicate that the undular weir flow is two-dimensional. The smallest flow depth (on the crest) is observed always upstream of the first wave crest (Fig. 1B), and the undulations propagate over the entire crest.

Further, the writer reanalysed the characteristics of free-surface undulations downstream of the first wave crest for undular weir flows (Table 4). The data are plotted in Fig. 4, where Δd and L_w are respectively the wave amplitude and the wavelength of the first wavelength (see Fig. 1B). The results are compared with undular jump data and with the solution of the Boussinesq equation for the undular surge (Andersen 1978).

Figure 4 indicates that the free-surface undulation characteristics for undular weir flows are similar to those for undular hydraulic jumps and undular surges in prismatic channels. Further, the relationship between wave amplitude and approach flow Froude number, Fr_1, exhibits the same shape as undular hydraulic jumps (Fig. 4A):

1. For Froude numbers close to unity, the data follow closely the theoretical solution of the Boussinesq equation, and the wave amplitude is about $\Delta d/d_c = 0.73(Fr_1 - 1)$.
2. With increasing Froude numbers, the wave amplitude data start diverging from the Boussinesq equation solution and reach a maximum value.
3. For large Froude numbers, the wave amplitude decreases with increasing Froude numbers as shown by Hager and Schwalt (1994) in their figure 8*a*.

In Fig. 4B, the data of Hager and Schwalt (1994) could be misread. With their data, the wavelength appears to increase with increasing Froude numbers. But an increase of Froude number brings also an increase of the aspect ratio d_c/W. Figure 4B suggests therefore an increase of wavelength with increasing aspect ratio, i.e., as for undular hydraulic jump flows (Chanson and Montes 1995).

3.3. Discussion

In Fig. 4, some data are plotted for subcritical Froude numbers. In these cases, supercritical flow conditions were not observed at all. The data are reported for completeness.

A particular feature of undular weir flow is the developing boundary layer along the flat crest. The boundary layer development is a function of the upstream edge shape. Isaacs (1981) discussed specifically the effects of the boundary layer for a broad-crested weir.

Undular weir flows occur always for low flow depth and the effects of the boundary layer cannot be ignored. Further, the rapid pressure and velocity redistributions at the upstream end of the sill modify substantially the upstream flow properties. For these reasons, the analogy between undular weir flow and undular jump or undular surge should be limited.

4. Free-surface undulations downstream of a backward-facing step and related cases

4.1. Undular flow downstream of drop

Undular flows are observed sometimes downstream of backward-facing steps, i.e., drops (Fig. 1C). Hager and Kawagoshi (1990) showed excellent photographs of undular flow downstream of rounded-edge drops. Several researchers (Table 5) proposed criterion for the establishment of free-surface undulations.

The author reanalysed the characteristics of undular flow downstream of backward-facing steps. The experimental flow conditions are summarized in Table 6. Figure 5 presents a comparison between wave amplitude data and ideal fluid flow calculations. A similar trend is observed, but the data of wave amplitude are smaller than undular surge results.

Fig. 4. Free-surface undulations characteristics: comparison between undular weir flows (Table 4), undular flow in the barrel of a minimum energy loss (MEL) culvert (present study, Table 8), undular jump flow (Chanson 1993), and undular surge theory (Andersen 1978). (A) dimensionless wave amplitude $\Delta d/d_c$; (B) dimensionless wavelength L_w/d_c.

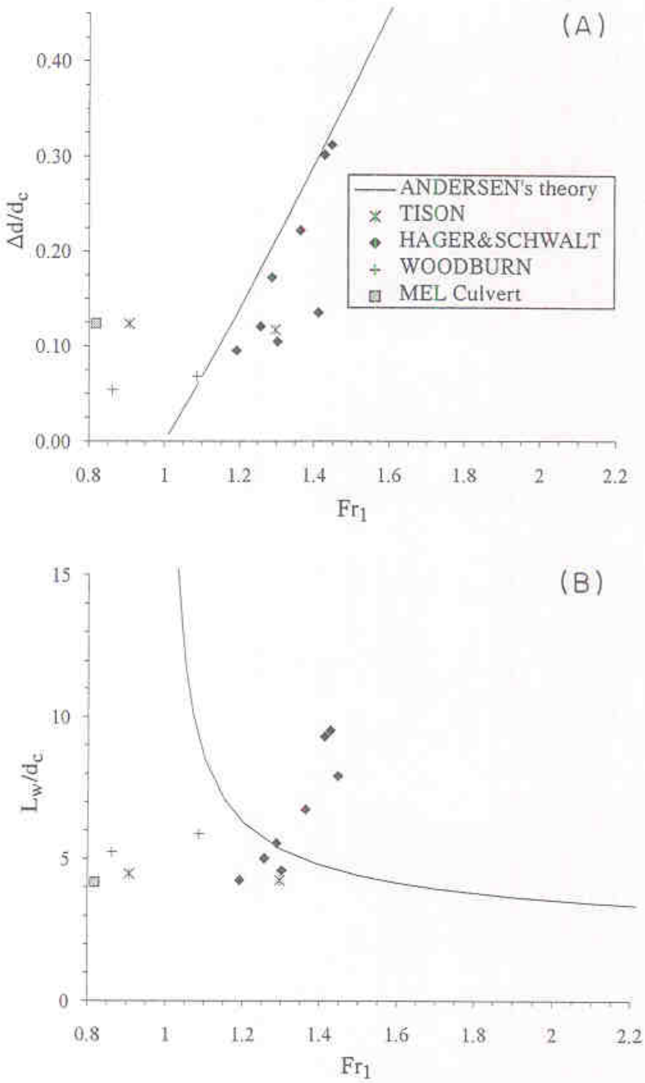

4.2. Related cases

Other flow situations can be related to the flow downstream of a drop (Figs. 1D and 1E). These are the flow downstream of an impinging jet, the flow downstream of a submerged body, and the flow downstream of a submerged sharp-crested weir. In each case, the flows impinge a downstream subcritical flow as a slightly inclined planar jet and the downstream free-surface undulations form above a developing shear layer/wake region (Fig. 1F). The flow conditions for the existence of undular flow are summarized in Table 5. It is interesting to note the reasonably close agreement between the various criteria despite the different geometries.

Wave amplitude and wavelength data are reported in Figs. 5–8. Details of the experimental flow conditions are given in Table 6. Figures 5 and 6 show the wave parameters as functions of the impinging jet Froude number. The characteristics of undular flow downstream of a submerged body are presented in Figs. 7 and 8, where the Froude number is defined as that satisfying the Bélanger equation for the measured ratio d_1/d_2, where d_1 is the minimum flow depth upstream of the first wave crest (Figs. 1D and 1E) and d_2 is the downstream flow depth.

The wave amplitude data compare well with ideal fluid flow calculations. Some discrepancies are noted between wavelength data and Andersen's (1978) calculations.

5. Undular flow in culverts

5.1. Presentation

A culvert is a covered channel of relatively short length to pass waters through an embankment (e.g., highway). Most culverts consist of three parts: the intake (or "fan"), the barrel, and the diffuser. The design varies from a simple geometry (i.e., box culvert) to a hydraulically smooth shape (i.e., MEL culvert[3]) (Fig. 9).

A culvert is designed normally to operate as an open channel. The basic principle of the culvert is to induce critical flow conditions in the barrel in order to maximize the discharge per unit width and to reduce the barrel cross section.

The flow upstream and downstream of the culvert is subcritical typically. As the flow approaches the culvert, the constriction (i.e., intake section) induces an increase in Froude number. For the design discharge, the flow becomes near-critical in the barrel. In practice, perfect-critical flow conditions in the barrel are difficult to establish; they are characterized by "choking" effects and free-surface instabilities. Usually, the Froude number in the barrel is about 0.7 to 0.9.

5.2. Hydraulic design of culvert

A culvert is designed for a specific flow rate. Its hydraulic performances are the maximum discharge Q_w^{max} (i.e., design discharge) and the maximum head loss ΔH. Substantial head losses might induce upstream backwater effects and must be minimized.

The hydraulic calculations are based upon the assumptions of smooth intake and diffuser, no (or minimum) energy loss, and critical flow conditions in the barrel. For a rectangular cross section, the maximum discharge per unit width is achieved for critical flow conditions:

$$[9] \quad q_w^{max} = \sqrt{g}\left[\frac{2}{3}(E_o + \Delta z - \Delta H)\right]^{3/2}$$

The minimum barrel width for critical flow conditions is then

$$[10] \quad W_{min} = \frac{Q_w^{max}}{\sqrt{g}}\left[\frac{2}{3}(E_o + \Delta z - \Delta H)\right]^{-3/2}$$

where E_o is the upstream specific energy, Δz the bed elevation difference between the upstream channel and the barrel bottom (Fig. 9), and ΔH the head loss.

Equation [10] gives the minimum barrel width to obtain near-critical flow without choking effects. It shows that the barrel width can be reduced by lowering the barrel bottom

[3] The design of a minimum energy loss (MEL) culvert is associated with the concept of constant total head. The inlet and outlet must be streamlined in such a way that significant form losses are avoided. For a complete review of minimum energy loss culverts, see Apelt (1983).

Table 5. Conditions for free-surface undulations downstream of backward-facing steps and weirs.

Reference	d_c/W	Flow conditions	Remarks
		Undular flow downstream of rounded drop	
Sharp (1974)		$Fr_1 < 2.2$ for $\Delta z/d_1 = 2$ $Fr_1 < 4$ for $\Delta z/d_1 = 3.5$	Laboratory experiments*
Hager and Kawagoshi (1990)	0.03–0.135	$Fr_1 < 2.44 + 0.28\ \Delta z/d_1$	Laboratory experiments*
		Undular flow downstream of abrupt drop	
Chow (1959)		$\frac{1}{2}\frac{d_2}{d_1 - d_2}\left[1 - \left(\frac{d_2}{d_1} - \frac{\Delta z}{d_1}\right)\right]^2 < Fr_1^2 < \frac{1}{2}\frac{d_2}{d_1 - d_2}\left[\left(1 + \frac{\Delta z}{d_1}\right)^2 - \left(\frac{d_2}{d_1}\right)^2\right]$	*
		Undular flow downstream of sharp-crested weir	
Bazin (1888–1898)		$(d_1 - d_2)/\Delta z < \frac{1}{6}$ to $\frac{1}{5}$ †	Large-scale experiments
		Undular flow downstream of weir with circular crest	
Rehbock (1929)		$0.18 < (d_1 - d_2)/\Delta z < 0.233$ †	Laboratory experiments ($q_w = 0.027$ m²/s, $\Delta z = 0.15$ m)
		Undular flow downstream of plane plunging jet	
Sene (1984)	0.0073, 0.0358	$10° <$ jet angle $< 30°$	Laboratory experiments
		Undular flow downstream of submerged body	
Duncan (1983)		$\Delta z/d_o < 0.132$ for $V = 0.8$ m/s	Laboratory experiments‡
Voutsis and McKinnon (1994)	0.299, 0.311	$\Delta z/d_o < 0.47$	Laboratory experiments‡

*See Fig. 1 for the definition of symbols.
† d_1 and d_2 are the flow upstream and downstream depths measured above the weir crest.
‡ See Fig. 1 and Table 6 for the definition of symbols and additional information.

Table 6. Experiments with backward-facing steps and related cases.

Reference	q_w (m²/s)	d_1 (m)	Fr_1	d_c/W	Upstream flow*	Comments
			Undular jump downstream of rounded drop			
Sharp (1974)	—	—	—	—	P/D	$W = 0.203$ m‡
Hager and Kawagoshi (1990)	—	—	—	0.03–0.135	P/D	$W = 0.5$ m‡
			Undular flow downstream of plane plunging jet			
Sene (1984)	0.0073, 0.0359	0.006–0.016	3.2–7.7†	0.1099, 0.3177		Bidimensional jet (jet angle between 10° and 30°)†; $W = 0.16$ m
			Undular flow downstream of submerged body			
Duncan (1983)	0.6–1 m/s (foil speed)	0.3–0.45			At rest	NACA 0012-shape hydrofoil moving in a 24-m-long flume ($W = 0.61$ m); foil at 0.175 m above the tank bottom
Voutsis and McKinnon (1994)	0.064			0.299	P/D	T-piece model;‡ $W = 0.25$ m
	0.064, 0.068			0.299, 0.311	P/D	4-girder (AASHTO IV) concrete bridge model;‡ $W = 0.25$ m

*Upstream flow conditions: F/D, fully developed boundary layer; P/D, partially developed boundary layer.
† Jet Froude number defined in terms of the jet thickness.
‡ See Fig. 1 for the definition of symbols.

Fig. 5. Dimensionless wave amplitude of undular flow downstream of drop and inclined jet. Fr_1 is defined in Fig. 1D. Comparison between undular surge theory (Andersen 1978) and experimental data (Table 6).

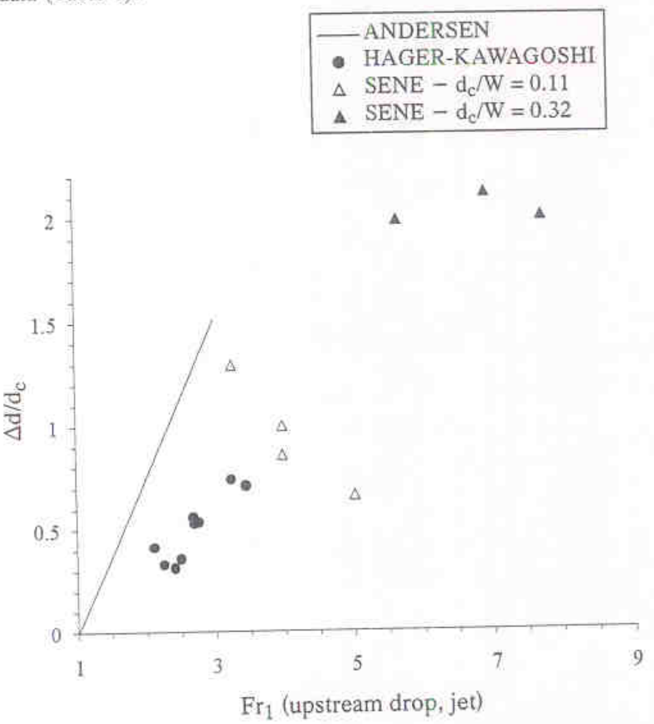

Fig. 6. Dimensionless wavelength of undular flow downstream of an inclined jet. Fr_1 is defined in Fig. 1D. Comparison between undular surge theory (Andersen 1978) and experimental data (Table 6).

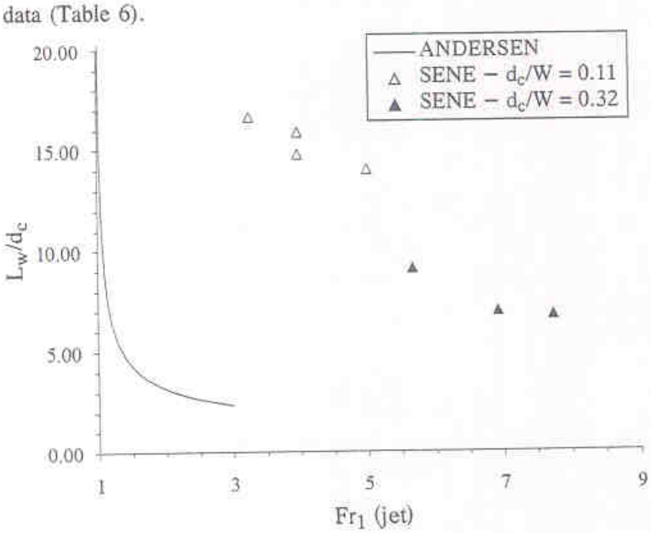

elevation. Designers must, however, choose an adequate barrel width to avoid the risks of culvert obstruction by debris (e.g., rocks and trees).

5.3. Undular flow in the barrel

In the barrel, the near-critical flow at design discharge is characterized by the establishment of stationary free-surface undulations (e.g., Fig. 10). For the designers, the charac-

Fig. 7. Dimensionless wave amplitude of undular flow downstream of a submerged body. Fr is the Froude number satisfying the Bélanger equation for the measured ratio d_1/d_2 (as defined in Fig. 1E). Comparison between undular surge theory (Andersen 1978) and experimental data (Table 6).

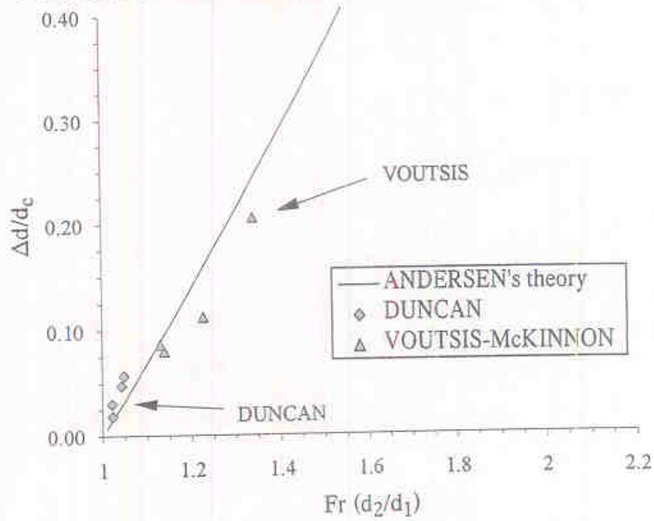

Fig. 8. Dimensionless wavelength of undular flow downstream of a submerged body. Fr is the Froude number satisfying the Bélanger equation for the measured ratio d_1/d_2 (as defined in Fig. 1E). Comparison between undular surge theory (Andersen 1978) and experimental data (Table 6).

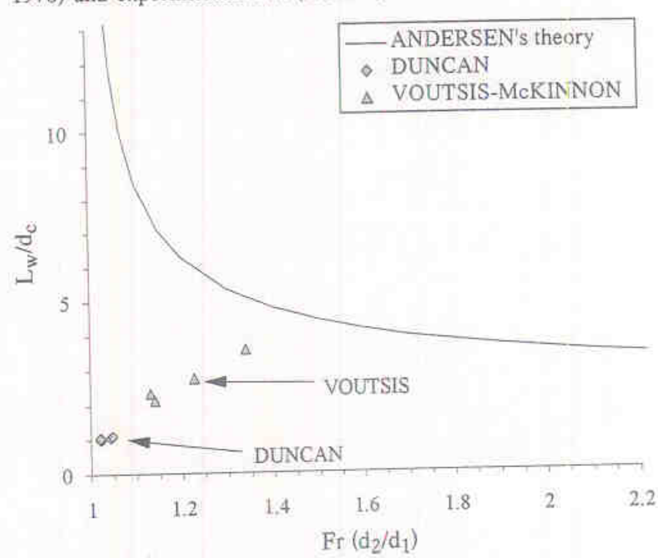

teristics of the free-surface undulations are important for the sizing of the culvert height. Henderson (1966) recommended that the upstream head over barrel height ratio should be less than 1.2 for the establishment of free-surface flow in the barrel. Such a ratio gives a minimum clearance above the free-surface level in the barrel of about 20%.

Two culvert experiments are performed in the Hydraulics/Fluid Mechanics Laboratory of the University of Queensland: a box culvert model and a MEL culvert model (Table 7). For the design discharge (i.e., 0.01 m^3/s), undular flows are clearly observed in the barrel of both models. In each case,

Fig. 9. Sketch of culverts. (MEL, minimum energy loss.)

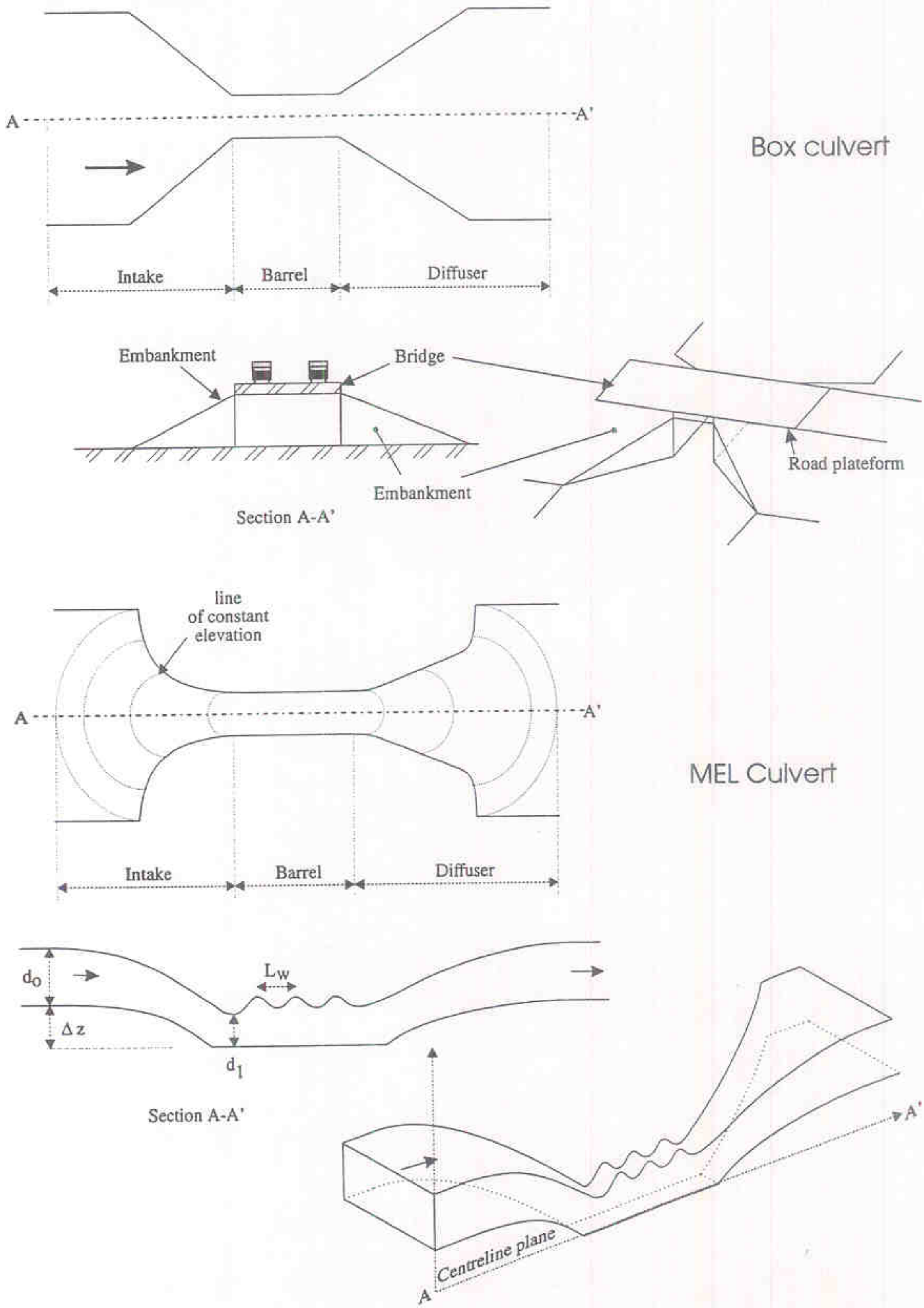

the free-surface undulations are two-dimensional.

For the MEL culvert experiment, the maximum free-surface height in the barrel is about 20% above the mean free-surface level. Further, the free-surface undulation characteristics are very close to undular weir flow (Fig. 4). Both the broad-crested weir and the culvert are designed specifically for near-critical flow above the crest and in the barrel, respectively. It is therefore justified to compare their wave

Fig. 10. Longitudinal free-surface profile in the barrel of the minimum energy loss culvert.

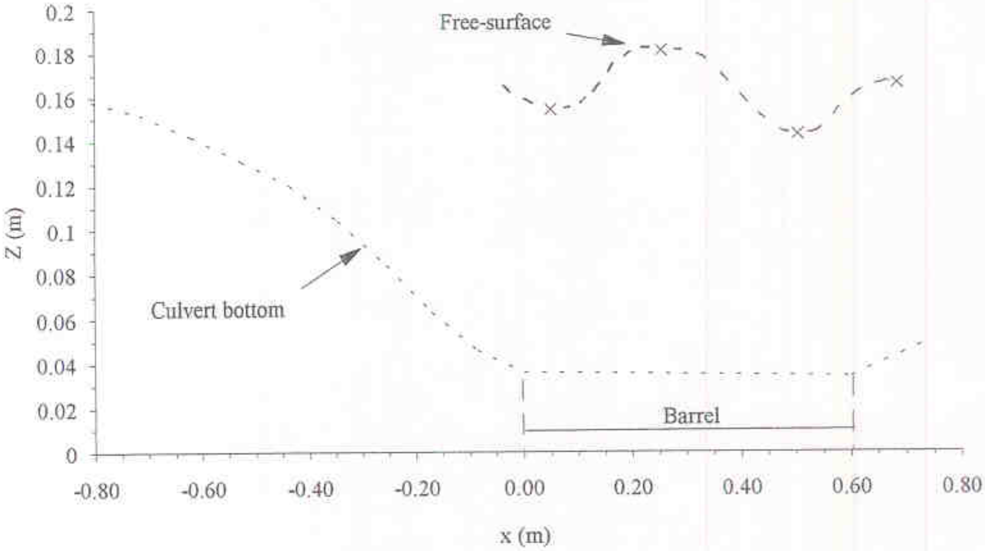

Table 7. Culvert experiments — present study.

Experiment	Design discharge Q_w^{max} (m^3/s)	Barrel dimension Width, W_{min} (m)	Height (m)	Length (m)	Remarks
Box culvert	0.01	0.15	0.11	0.5	Upstream channel width, 1 m; intake and exit, 45° diffuser; Δz = 0; E_o/d_c = 1.915; Fr_o = 0.431
MEL culvert*	0.01	0.10	0.17	0.6	Upstream channel width, 1 m; Δz = 0.14 m; E_o/d_c = 1.915; Fr_o = 0.431

*MEL, minimum energy loss.

properties as shown in Fig. 4. Note that undular weir flows are usually thin nappes affected by the developing bottom boundary layer, while the barrel of a culvert is usually narrow inducing thick flows which are affected by developing bottom and sidewall boundary layers.

6. Summary and conclusion

The present study develops a reanalysis of near-critical flows and a comparison with recent undular jump flow experiments. For Froude numbers slightly above unity, the characteristics of the free-surface undulations are comparable in most near-critical flow situations. And ideal-fluid flow theories (e.g., Keulegan and Patterson 1940; Andersen 1978) can predict reasonably well the wave properties. However, with increasing Froude numbers, each type of near-critical flows exhibits a different behaviour, e.g., the flow properties of undular hydraulic jumps (Chanson 1993, 1995) cannot be predicted with ideal-fluid theories for larger Froude numbers.

The similarity between the various types of near-critical flows might provide some order of magnitude for free-surface undulations at near-critical flows. The generalization of the results should currently not be extended to precise calculations. The basic flow patterns are strongly affected by the upstream flow conditions, the wall friction, and the related developing boundary layers, and by possible flow separation and wake region (e.g., downstream of a backward-facing step).

The study has highlighted the lack of experimental data and some limitations of ideal-fluid flow theories. It is hoped that new investigations will follow to provide additional information for hydraulic engineers.

Acknowledgements

The author thanks his colleagues Professor C.J. Apelt and Dr. D.K. Brady, the University of Queensland, Australia, for their contributions to this study.

References

Andersen, V.M. 1978. Undular hydraulic jump. ASCE Journal of the Hydraulic Division, **104**(HY8): 1185–1188. Discussion: **105**(HY9): 1208–1211.

Apelt, C.J. 1983. Hydraulics of minimum energy culverts and bridge waterways. Australian Civil Engineering Transactions, Institution of Engineers, Australia, **CE25**(2): 89–95.

Bazin, H. 1865. Recherches expérimentales sur la propagation des ondes. (Experimental research on wave propagation.) Memoirs, Académie des sciences, Paris, France, **19**: 495–644. (In French.)

Bazin, H. 1888–1898. Expériences nouvelles sur l'ecoulement par déversoir. (Recent experiments on the flow of water over weirs.) Annales des ponts et chaussées, mémoires et documents, Paris, France, 1888: Ser. 6, No. 16, pp. 393–448; 1890: Ser. 6, No. 19, pp. 9–82; 1891: Ser. 7, No. 2, pp. 445–520; 1894: Ser. 7, No. 7, pp. 249–357; 1896: Ser. 7, No. 12, pp. 645–731; 1898: Ser. 7, No. 15, pp. 151–264. (In French.)

Benet, F., and Cunge, J.A. 1971. Analysis of experiments on secondary undulations caused by surge waves in trapezoidal channels. Journal of Hydraulic Research, International Association for Hydraulic Research, **9**(1): 11–33.

Bos, M.G. 1976. Discharge measurement structures. Publication No. 161, Delft Hydraulic Laboratory, Delft, The Netherlands, (also Publication No. 20, ILRI, Wageningen, The Netherlands).

Boussinesq, J.V. 1871. Sur le mouvement permanent varié de l'eau dans les tuyaux de conduite et dans les canaux découverts. (On the steady varied flow of water in conduits and open channels.) Comptes rendus des séances de l'Académie des sciences, **73**: 101–105. (In French.)

Boussinesq, J.V. 1877. Essai sur la théorie des eaux courantes. (Essay on the theory of water flow. Memoirs, Académie des sciences, Paris, France, Ser. 3, **23**(1) supplement 24: 1–680. (In French.)

Chanson, H. 1993. Characteristics of undular hydraulic jumps. Department of Civil Engineering, University of Queensland, Australia, November, Research Report No. CE146.

Chanson, H. 1995. Flow characteristics of undular hydraulic jumps. Comparison with near-critical flows. Department of Civil Engineering, University of Queensland, Brisbane, Australia, June, Report CH45/95.

Chanson, H., and Montes, J.S. 1995. Characteristics of undular hydraulic jumps. Experimental apparatus and flow patterns. ASCE Journal of Hydraulic Engineering, **121**(2): 129–144.

Chow, V.T. 1959. Open channel hydraulics. McGraw-Hill International, New York, N.Y.

Duncan, J.H. 1983. The breaking and non-breaking wave resistance of a two-dimensional hydrofoil. Journal of Fluid Mechanics, **126**: 507–520.

Favre, H. 1935. Etude théorique et expérimentale des ondes de translation dans les canaux découverts. (Theoretical and experimental study of travelling surges in open channels.) Dunod edition, Paris, France. (In French.)

Gordienko, P.I. 1978. Reinforced-concrete-earth overflow dams. Dams & Spillways, Collection of Works No. 61, Issue 2, MISI, Moscow, pp. 3–17. (In Russian.)

Govinda Rao, N.S., and Muralidhar, D. 1963. Discharge characteristics of weirs of finite-crest width. Journal La Houille Blanche, August/September, No. 5, pp. 537–545.

Hager, W.H. 1995. Undular bores (favre-waves) in open channels — experimental studies. Discussion. Journal of Hydraulic Research, International Association for Hydraulic Research, **33**(3): 274–277.

Hager, W.H., and Kawagoshi, N. 1990. Hydraulic jumps at rounded drop. Proceedings of the Institution of Civil Engineers, Part 2, **89** (December): 443–470.

Hager, W.H., and Schwalt, M. 1994. Broad-crested weir. ASCE Journal of Irrigation and Drainage Engineering, **120**(1): 13–26. Discussion: **121**(2): 222–226.

Henderson, F.M. 1966. Open channel flow. MacMillan Company, New York, N.Y.

Isaacs, L.T. 1981. Effects of laminar boundary layer on a model broad-crested weir. Department of Civil Engineering, University of Queensland, Brisbane, Australia, Research Report No. CE28.

Keulegan, G.H., and Patterson, G.W. 1940. Mathematical theory of irrotational translation waves. Journal of Research of the National Bureau of Standards, RP1273, U.S. Department of Commerce, **24**(1): 47–101.

Kurganov, A.M. 1974. Waves during near-critical flow in rectangular, triangular and parabolic sections. Izvestiya Vysshikh Uchebnykh Zavedenii, Stroitel'stvo i Arkhitektura, No. 6, pp. 129–135. (In Russian.)

Rehbock, T. 1929. The River Hydraulic Laboratory of the Technical University of Karlsruhe. *In* Hydraulic laboratory practice. American Society of Mechanical Engineers, New York, N.Y. pp. 111–242.

Rouse, H. 1938. Fluid mechanics for hydraulic engineers. McGraw-Hill, New York, N.Y.

Sandover, J.A., and Holmes, P. 1962. The hydraulic jump in trapezoidal channels. Water Power, November, pp. 445–449.

Sene, K.J. 1984. Aspects of bubbly two-phase flow. Ph.D. thesis, Department of Civil Engineering, Trinity College, Cambridge, United Kingdom.

Serre, F. 1953. Contribution à l'etude des ecoulements permanents et variables dans les canaux. (Contribution to the study of permanent and non-permanent flows in channels.) Journal La Houille Blanche, December, pp. 830–872. (In French.)

Sharp, J.J. 1974. Observations on hydraulic jumps at rounded steps. ASCE Journal of the Hydraulic Division, **100**(HY6): 787–795.

Tison, L.J. 1950. Le déversoir epais. (Broad-crested weir.) Journal La Houille Blanche, pp. 426–439. (In French.)

Treske, A. 1994. Undular bores (favre-waves) in open channels — experimental studies. Journal of Hydraulic Research, International Association for Hydraulic Research, **32**(3): 355–370. Discussion: **33**(3): 274–278.

Tricker, R.A.R. 1965. Bores, breakers, waves and wakes. American Elsevier Publishing Co., New York, N.Y.

Tursunov, A.A. 1969. Subcritical state of free-surface flows. Izvestiya Vsesoyuznogo Nauchno-Issledovatel'skogo Instituta Gidrotekhniki, **90**: 201–223. (In Russian.)

Voutsis, A., and McKinnon, D. 1994. Hydrodynamic and debris forces on fully and partially submerged bridge superstructures. B.Eng. thesis, Department of Civil Engineering, University of Queensland, Brisbane, Australia.

Woodburn, J.G. 1932. Tests of broad-crested weirs — Discussion. Transactions, American Society of Civil Engineers, **96**: 447–453.

Zienkiewicz, O.C., and Sandover, J.A. 1957. The undular surge wave. Proceedings of the 7th International Association for Hydraulic Research Congress, Lisbon, Portugal, Vol. II(D25), pp. D1–11.

List of symbols

A	cross-section area (m^2); for a rectangular channel, $A = Wd$
C_s	surge celerity (m/s) as seen by an observer standing on the channel bank
d	flow depth (m) measured perpendicular to the channel bottom
d_c	critical flow depth (m); for a rectangular channel, $d_c = \sqrt[3]{q_w^2/g}$
d_o	flow depth (m) upstream of a hydraulic obstacle (e.g., weir, submerged body)
E	specific energy (m)
E_o	mean specific energy (m) upstream of a hydraulic obstacle (e.g., weir, submerged body)
Fr	Froude number; for steady open channel flow, $\mathrm{Fr} = V/\sqrt{gA/W}$; surge Froude number: $\mathrm{Fr} = (V - C_s/\sqrt{gA/W}$
Fr_o	Froude number upstream of a hydraulic obstacle (e.g., culvert)
g	gravity constant; $g = 9.80$ m/s^2 in Brisbane, Australia

L_w wavelength (m)
Q_w water discharge (m^3/s)
Q_w^{max} maximum water discharge (m^3/s) for a given specific energy, i.e., water discharge at critical flow conditions
q_w water discharge per unit width (m^2/s)
q_w^{max} maximum water discharge per unit width (m^2/s) for a given specific energy, i.e., water discharge at critical flow conditions
V velocity (m/s)
W channel width (m); for a channel of irregular cross section, W is the free-surface width
W_{min} minimum design width (m) of a culvert barrel
x longitudinal distance (m) measured along the channel bottom
α channel slope
Δd wave amplitude (m)
ΔH head loss (m)
Δz drop height (m)

Subscript

1 flow conditions upstream of the hydraulic jump; initial flow conditions before the passage of a positive surge
2 flow conditions downstream of the hydraulic jump; new flow conditions after the passage of a positive surge